The modifying enzyme Tsr3 establishes the hierarchy of Rio kinase binding in 40S ribosome assembly

HAINA HUANG,[1,2] MELISSA PARKER,[1,2] and KATRIN KARBSTEIN[1,2,3]

[1]Department of Integrative Structural and Computational Biology, The Scripps Research Institute, Jupiter, Florida 33458, USA
[2]Skaggs Graduate School of Chemical and Biological Sciences at Scripps Research, Jupiter, Florida 33458, USA
[3]HHMI Faculty Scholar, Chevy Chase, Maryland 20815, USA

ABSTRACT

Ribosome assembly is an intricate process, which in eukaryotes is promoted by a large machinery comprised of over 200 assembly factors (AFs) that enable the modification, folding, and processing of the ribosomal RNA (rRNA) and the binding of the 79 ribosomal proteins. While some early assembly steps occur via parallel pathways, the process overall is highly hierarchical, which allows for the integration of maturation steps with quality control processes that ensure only fully and correctly assembled subunits are released into the translating pool. How exactly this hierarchy is established, in particular given that there are many instances of RNA substrate "handover" from one highly related AF to another, remains to be determined. Here we have investigated the role of Tsr3, which installs a universally conserved modification in the P-site of the small ribosomal subunit late in assembly. Our data demonstrate that Tsr3 separates the binding of the Rio kinases, Rio2 and Rio1, with whom it shares a binding site. By binding after Rio2 dissociation, Tsr3 prevents rebinding of Rio2, promoting forward assembly. After rRNA modification is complete, Tsr3 dissociates, thereby allowing for recruitment of Rio1 into its functional site. Inactive Tsr3 blocks Rio1 function, which can be rescued using mutants that bypass the requirement for Rio1 activity. Finally, yeast strains lacking Tsr3 randomize the binding of the two kinases, leading to the release of immature ribosomes into the translating pool. These data demonstrate a role for Tsr3 and its modification activity in establishing a hierarchy for the function of the Rio kinases.

Keywords: quality control; ribosome assembly; RNA modification; Rio kinase; Tsr3

INTRODUCTION

Ribosomes are molecular machines composed of four ribosomal RNAs (rRNAs) and 79 ribosomal proteins. Assembly of these complexes occurs in a highly coordinated manner that starts cotranscriptionally in the nucleolus and is completed in the cytoplasm. This process is assisted by over 200 assembly factors (AFs), which transiently bind the nascent subunits to facilitate the modification, processing, and folding of the rRNAs, promote the incorporation of ribosomal proteins, and allow for regulation and quality control (Woolford and Baserga 2013; de la Cruz et al. 2015; Peña et al. 2017; Chaker-Margot 2018; Bassler and Hurt 2019; Klinge and Woolford 2019).

Structural and biochemical studies of ribosome assembly have yielded substantial insight into these molecular events. While parallel assembly pathways appear to play a role during very early stages of assembly (Mulder et al. 2010; Sashital et al. 2014; Davis et al. 2016; Sanghai et al. 2018; Cheng et al. 2019, 2020; Du et al. 2020), the process overall is highly hierarchical. For example, during the latest cytoplasmic stages of 40S assembly, the remaining AFs dissociate in a highly ordered manner (Ghalei et al. 2015, 2017; Parker et al. 2019; Huang et al. 2020). This hierarchy allows for the integration of quality control with progress in the assembly cascade and is thus critical for faithful assembly. How this hierarchy is achieved is not well understood.

As part of the hierarchical assembly pipeline, there are numerous instances where the same site is bound by a succession of AFs: for example, Krr1 and Pno1 bind the same location on the platform in early and late intermediates (Sturm et al. 2017); Bms1 and Tsr1 occupy the same site on the body in early and late intermediates (Gelperin et al. 2001; Kornprobst et al. 2016; McCaughan et al. 2016); and, finally, the kinases Rio2 and Rio1 share a binding site on the head in late and very late intermediates

Corresponding author: kkarbst@scripps.edu
Article is online at http://www.rnajournal.org/cgi/doi/10.1261/rna.078994.121.

(Strunk et al. 2011; Ameismeier et al. 2020). Further complicating the establishment of hierarchy, both Krr1 and Pno1 harbor two conserved KH domains and a nearly identical overall structure (Sturm et al. 2017); Tsr1 is an inactive structural mimic of the GTPase Bms1 (Gelperin et al. 2001; Strunk et al. 2011; McCaughan et al. 2016) and Rio1 and Rio2 share features of the RIO kinase domain (Knuppel et al. 2018). How the order in which these factors bind (and thus function) is established remains unknown. This is especially important for factors that release others, like Rio1, which dissociates Nob1 and Pno1 (Turowski et al. 2014; Belhabich-Baumas et al. 2017; Parker et al. 2019; Ameismeier et al. 2020; Plassart et al. 2021). Premature binding of Rio1 (prior to Rio2) would lead to the release of immature rRNA into the translating pool, which changes the proteome. Similarly, how rebinding of the earlier factor after its dissociation is avoided also remains unclear.

To address these questions, we have studied the temporal ordering in the binding and activity of the kinases Rio2 and Rio1, which are 19% identical and 43% similar, and whose structures overlap with a root mean square deviation (RMSD) of 1.6 Å (archaeal structures) or 3.4 Å (human structures). Rio1 and Rio2 also share a binding site on the head of the nascent 40S subunit (Fig. 1A; Supplemental Fig. S1). Rio2 binds first in the late nucleolar stage of assembly (Fig. 1B; Geerlings et al. 2003; Strunk et al. 2011; Ferreira-Cerca et al. 2012). Its dissociation requires both its ATPase activity (Ferreira-Cerca et al. 2012) as well as the prior dissociation of the assembly factors Ltv1 and Enp1, which appears to promote changes in the head (Heuer et al. 2017; Scaiola et al. 2018; Huang et al. 2020). These adjustments in the head structure also require the correct positioning of the ribosomal protein Rps15, mutations in which also block release of Rio2, but not Ltv1 or Enp1 (Huang et al. 2020). Rio2 dissociation

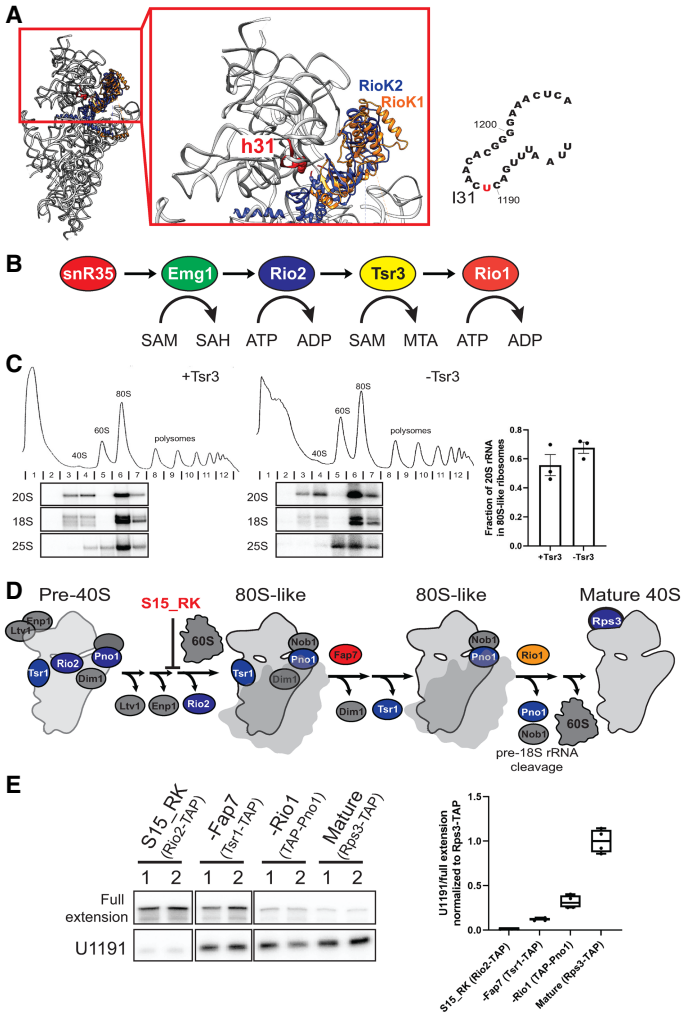

FIGURE 1. Tsr3 functions in 80S-like ribosomes. (*A*) (*Left*) Superimposition of two human pre-40S structures (PDBID 6ZXE and 6G18, respectively) based on Rps15 (uS19) shows overlap of human Rio1 (RioK1, colored in orange) and human Rio2 (RioK2, colored in blue). 18S rRNA from Rio1 containing pre-40S (PDBID 6ZXE) is shown in gray ribbon, with h31 highlighted in red and U1248 (U1191 in yeast) highlighted in red sphere. (*Right*) Secondary structure of 18S loop 31 (l31), which is bound by all factors during assembly and contains the snR35, Emg1, and Tsr3 modification site at U1191. (*B*) snR35, Emg1, Rio2, Tsr3, and Rio1 all bind loop 31 at successive stages of 40S maturation. Emg1 and Tsr1 use *S*-adenosyl-methionine (SAM) to produce *S*-adenosyl-homocysteine (SAH) or methylthioadenosine (MTA), respectively, while Rio2 and Rio1 hydrolyze ATP. (*C*) Absorbance profiles at 254 nm and corresponding northern blots of 10%–50% sucrose gradients from Gal:Fap7 (+Tsr3) or ΔTsr3, Gal:Fap7 (−Tsr3) cells. In all cases, Fap7 was depleted in glucose for over 16 h to accumulate 80S-like ribosomes. Fractions 2–7 for each gradient were probed for 20S, 18S, and 25S rRNA. Quantifications of the data on the *left* indicate the efficiency of formation of 80S-like ribosomes. Data are shown as mean with standard deviation ($n = 3$). (*D*) Simplified scheme showing ordered release of Ltv1, Enp1, and Rio2 (blocked by Rps15_RK) before formation of 80S-like ribosomes and different 80S-like ribosomes that accumulate in the absence of Fap7 and Rio1, respectively. Tagged proteins for pull-downs are indicated in blue. Note that Rps3 is bound in all the stages depicted here, but because mature 40S are so much more abundant the majority of Rps3-TAP-tagged subunits are mature. (*E*) (*Left*) Primer extension results indicating the installation of acp modification at U1191 in different purified pre-40S intermediates and mature 40S. Signal for U1191 was first normalized to full extension before further normalization to mature 40S (Rps3-TAP). Two representative biological replicates (1, 2) are shown for each cell type. (*Right*) Quantification of the normalized U1191 stop from the *left* and two additional replicates ($n = 4$). Endogenous Rps15, Fap7, and Rio1 were depleted by growth in glucose of cells containing the respective proteins under the GAL-promoter. In the case of Rps15_RK, these cells were supplemented with a plasmid encoding Rps15_RK (Huang et al. 2020).

allows the nascent 40S subunits to enter a translation-like quality control cycle (Ferreira-Cerca et al. 2012; Huang et al. 2020), in which maturation is coupled to a test drive that probes the functionality of the newly made subunit (Lebaron et al. 2012; Strunk et al. 2012). At the very end of this translation-like cycle, after Nob1-dependent maturation of the 3′-end of 18S rRNA, Rio1 releases both Nob1 and its binding partner Pno1, thereby allowing for the incorporation of Rps26, the final step in maturation of the 40S subunit (Turowski et al. 2014; Belhabich-Baumas et al. 2017; Parker et al. 2019; Ameismeier et al. 2020; Plassart et al. 2021). How cells coordinate the activity of the two kinases to ensure that Rio2 acts before Rio1 and that Rio1 only binds after the translation-like quality control cycle is completed and not before or immediately after Rio2 remains unknown.

Rio1 and Rio2 both interact with a conserved rRNA loop in the P-site, loop 31 (l31), which closes helix 31 (h31, Fig. 1A). U1191 within this loop is modified in three steps, first by snR35-mediated conversion of the U to pseudouridine (Liang et al. 2009), followed by Emg1/Nep1-dependent methylation of the N1 nitrogen (Meyer et al. 2011; Thomas et al. 2011). The final step involves transfer of an amino-carboxypropyl (acp)-group to the N3 nitrogen catalyzed by the conserved modifying enzyme Tsr3 (Meyer et al. 2016). Thus, all these enzymes share the same binding site, and indeed snR35, Emg1, and Rio2 all have roles in preventing the premature formation of the loop structure (Huang and Karbstein 2021). Nonetheless, snR35 and Emg1 function cotranscriptionally in the nucleus, while Rio2, Tsr3, and Rio1 function in the cytoplasm. Here, we use structural, biochemical, and genetic tools, to show how Tsr3 separates the activity of the Rio2 and Rio1 kinases and helps ensure their sequential function. We first pinpoint the functional timing of Tsr3: after Rio2 dissociates but before Rio1 associates. Genetic interactions and biochemical data strongly suggest a role for Tsr3 in preventing rebinding of Rio2 to ensure its release is irreversible. Our data also reveal that the modification activity of Tsr3 is required for its release from pre-40S intermediates and that its dissociation is required for Rio1 binding. Deletion of Tsr3 leads to release of immature pre-18S rRNA into the polysomes, demonstrating the importance of Tsr3 in regulating the timing of Rio1 function.

RESULTS

Tsr3 functions in 80S-like ribosomes

Immunofluorescence experiments indicate that Tsr3 resides mostly in the cytosol (Breker et al. 2013, 2014). (A localization atlas of the yeast proteome is available at www.weizmann.ac.il/molgen/loqate.) Consistently, deletion of Tsr3 leads to accumulation of the cytoplasmic pre-18S rRNA precursor, 20S rRNA (Meyer et al. 2016). During the cytoplasmic stages of 40S ribosome maturation, a translation-like cycle serves as a mechanism for testing functionality of nascent 40S subunits (Lebaron et al. 2012; Strunk et al. 2012). Specifically, pre-40S intermediates are joined by mature 60S with the help of the translation initiation factor, eIF5B. The resulting 80S-like ribosomes do not produce proteins but serve as a hub for quality control and rRNA maturation. After that, 80S-like ribosomes are broken apart by the translation termination factor Rli1. Previous work indicated that Tsr3 acted around the time of formation of 80S-like ribosomes, as modification was not observed in assembly intermediates stalled just before formation of 80S-like ribosomes. Moreover, intermediates associated with eIF5B are the first to show the modification (Hector et al. 2014).

To more accurately pinpoint the timing of Tsr3 activity during 40S maturation, we first tested whether Tsr3 was required for the formation of 80S-like ribosomes. To answer this question, we used a previously described in vivo assay, in which we stall the translation-like cycle after the formation of 80S-like ribosomes by depleting the ATPase Fap7 using a galactose-inducible/glucose-repressible promoter (GAL-promoter) by growth in glucose (Strunk et al. 2012; Huang et al. 2020). The efficiency of 80S-like ribosome formation is measured by quantifying the fraction of 20S rRNA in 80S-like ribosomes. If a protein of interest is required for the formation of 80S-like ribosomes, then the fraction of 20S rRNA found in 80S-like ribosomes decreases, as the nascent subunits are stalled in 40S-sized intermediates. The fraction of 20S rRNA in 80S-like ribosomes does not decrease in Tsr3-deletion cells relative to wild-type (WT) cells. To the contrary, we observed a small increase in the fraction of 20S rRNA in 80S-like ribosomes (Fig. 1C). Together, these data demonstrate that deletion of Tsr3 does not interfere with 80S-like ribosome formation and suggest that Tsr3 functions within 80S-like ribosomes, such that its deletion exacerbates the Fap7-dependent block within 80S-like ribosomes.

We further dissected Tsr3's functional timing by asking when in the translation-like cycle its substrate is modified. As shown in the simplified scheme in Figure 1D, formation of 80S-like ribosomes requires the ordered release of the AFs Ltv1, Enp1, and Rio2 (Huang et al. 2020). Tsr1 and Dim1 dissociate from 80S-like ribosomes with the ATPase Fap7 releasing Dim1 (Ghalei et al. 2017). Finally, Pno1 and Nob1 are released by the kinase Rio1 after formation of mature 18S rRNA (Turowski et al. 2014; Parker et al. 2019; Ameismeier et al. 2020; Plassart et al. 2021). Guided by this scheme, we stalled assembly at distinct stages by depletion (using a GAL-promoter) or mutation of these AFs and then used TAP-tags on different assembly factors to isolate these 40S assembly intermediates. This is necessary to enrich the desired intermediates: for example, Rio2 cannot pull down 80S-like ribosomes because it dissociates prior to their formation. Moreover, in wild-type cells, all tagged assembly factors copurify a collection of intermediates, and depletion or mutation of assembly factors is

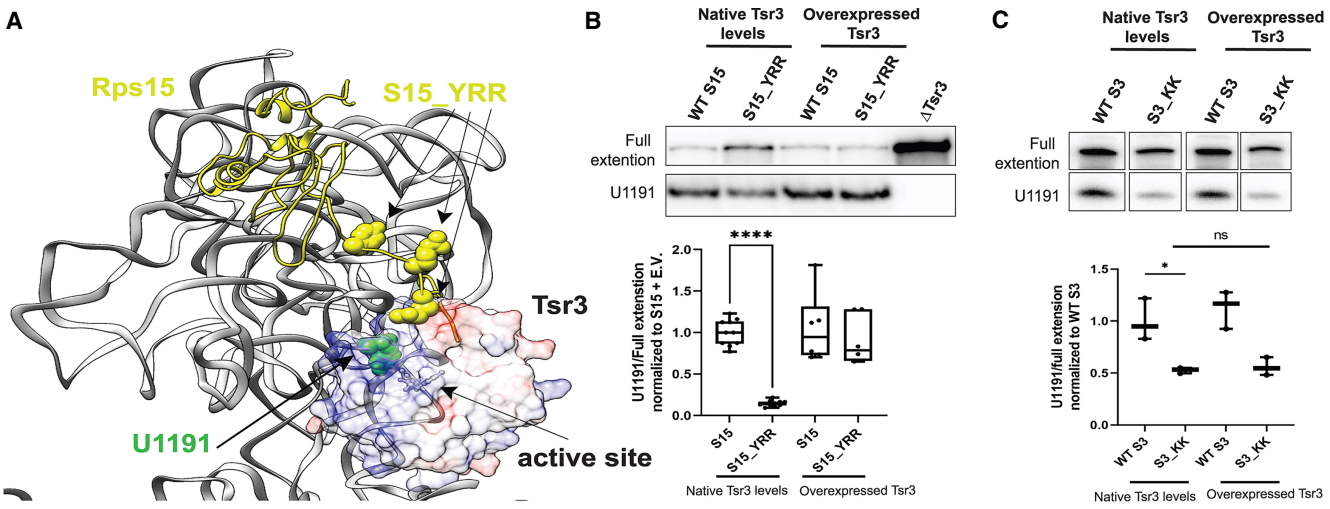

FIGURE 2. The Rps15 carboxy-terminal tail helps recruit Tsr3. (*A*) Predicted binding site of Tsr3 on 80S-like ribosomes. Pre-40S (PDBID: 6ZXE) and 80S-like (PDBID: 6WDR) ribosome structures were first overlayed based on 18S rRNA. The crystal structure of Tsr3 (PDBID: 5APG) was aligned to Rio1 from pre-40S (PDBID: 6ZXE) and then rotated so that its positively charged surface and its substrate-binding pocket face its rRNA substrate, U1191. 18S rRNA from 80S-like ribosome (PDBID: 6WDR) is shown in gray ribbon, with U1191 highlighted in green sphere. Rps15 from 80S-like ribosome is shown in yellow, with residues Y123, R127, and R130 highlighted in sphere. Tsr3 is shown as surface and colored based on charge (blue: positive; red: negative). The active site of Tsr3 is indicated by a black arrow based on its bound substrate analog, Se-adenosyl-selenomethionine. (*B*) (*Top*) Primer extension results show acp modification at U1191 of ribosomes from Gal:S15 cells supplemented with plasmids encoding WT S15 or S15_YRR and empty vector (EV) or Tsr3. (*Bottom*) Quantifications of the primer extension stop at U1191 relative to the full extension from the *top* and additional replicates. Significance was tested using one-way ANOVA (Sidak's multiple comparisons test). (****) $P_{adj} < 0.0001$; $n \geq 6$. (*C*) (*Top*) Primer extension results show acp modification at U1191 of ribosomes from Gal:Rps3 cells supplemented with plasmids encoding WT Rps3 or Rps3_KK and empty vector (EV) or Tsr3. (*Bottom*) Quantifications of the primer extension stop at U1191 relative to the full extension from the *top* and additional replicates. Significance was tested using one-way ANOVA (Sidak's multiple comparisons test). (*) $P_{adj} < 0.05$; $n = 3$.

required to enrich specific later intermediates and test whether these are modified.

To stall assembly immediately prior to release of Rio2 and the formation of 80S-like ribosomes, we used a previously described mutant in Rps15/uS19, S15_RK (R137E; K142, Huang et al. 2020) and isolated the intermediate using Rio2-TAP. Importantly, control experiments demonstrate that this mutation does not interfere with acp modification in mature 40S subunits (Supplemental Fig. S2A). To accumulate 80S-like intermediates prior to the release of Tsr1 and Dim1, we used Tsr1-TAP combined with depletion of Fap7 as previously described (Ghalei et al. 2017; Rai et al. 2021). Finally, to isolate assembly intermediates immediately prior to the release of Pno1 and Nob1, we depleted Rio1 and isolated the intermediates using a TAP-tag on Pno1 as also previously described (Parker et al. 2019). To purify mature 40S subunits, we used S3-TAP. The presence of the Tsr3-directed modification at U1191 leads to a stall during reverse transcription, which can be visualized as a prominent band in primer extension experiments (Meyer et al. 2016).

Intermediates stalled prior to Rio2 release and the formation of 80S-like ribosomes (Rps15_RK) do not show a substantial extension stop at U1191 (Fig. 1E; Supplemental Fig. S2B). Partial modification is observed in 80S-like ribosomes stalled prior to Fap7-dependent release of Dim1, which is further increased in intermediates stalled prior to Rio1 activity (Fig. 1E; Supplemental Fig. S2B). Together, these data strongly suggest that the modification occurs after Fap7-mediated release of Dim1 and before Rio1-dependent dissociation of Pno1 and Nob1. Thus, Tsr3 is recruited to nascent 40S ribosomes after Rio2 is released but before Rio1 is recruited. We suggest that the modification efficiency in the Rio1-depleted strain is less than in mature 40S because not all intermediates are stalled prior to the Rio1-dependent step due to a "backup" in the assembly line.

The Rps15 carboxy-terminal tail plays a direct role in recruiting Tsr3

To visualize how Tsr3 might be recruited to pre-ribosomes and gain insight into its potential interacting partner(s), we manually docked the Tsr3 crystal structure onto 80S-like ribosomes, placing its substrate-binding pocket and the RNA-binding surface (Meyer et al. 2016) toward its rRNA substrate, U1191 (Fig. 2A). This dock suggests that the carboxy-terminal extension of Rps15/uS19 might interact with Tsr3. We therefore tested whether mutations in the carboxy-terminal tail of Rps15 affect acp modification at U1191. For this experiment, we purified ribosomes from yeast cells where endogenous Rps15, expressed under a GAL-promoter, is depleted via growth in glucose, and

which are supplemented with plasmids encoding either wild-type Rps15 or the Rps15 mutant Rps15_YRR (Y123I, R127E, R130E). Using the primer extension assay described above on these mature ribosomes, we found a substantial defect in acp modification in ribosomes from yeast expressing Rps15_YRR relative to wild-type yeast (Fig. 2B), as predicted if the carboxy-terminal tail of Rps15 helps recruit Tsr3, similar to the docked model in Figure 2A. In contrast, neither the Rps15_RK nor the Rps15_EE (E110K, E118K) mutation affect Tsr3 modification (Supplemental Fig. S2A), demonstrating that the defect does not stem from impaired release of Rio2, and thus impaired recruitment of Tsr3, but has a different cause. If the reduced acp modification in the Rps15_YRR strain is due to defective Tsr3 recruitment, then we predict that overexpression of Tsr3 should rescue acp modification. Indeed, the modification defect introduced by S15_YRR can be almost entirely rescued by overexpression of Tsr3 (Fig. 2B), indicating a direct role for the Rps15 carboxy-terminal tail in recruiting Tsr3. To demonstrate that rescue of the acp modification defect by overexpression of Tsr3 is specific to Rps15_YRR and therefore reflective of direct effects in recruitment and not a generic feature of mutants defective in acp modification, we identified another mutant defective in acp modification, which is located on the solvent side and not the subunit interface where Tsr3 binds. The data in Figure 2C demonstrate that Rps3_KK (K7D, K10E) is also defective in acp modification. However, in contrast to Rps15_YRR, Rps3_KK's modification defect is not rescued by overexpression of Tsr3. Thus, together, these data suggest that the carboxy-terminal tail in Rps15, and specifically tyrosine 123 and arginines 127 and 130, are involved in the recruitment of Tsr3.

Tsr3 prevents rebinding of Rio2 to ensure its release is irreversible

Above, we have shown that Tsr3 is active after Rio2 release and prior to Rio1 recruitment. Moreover, all three enzymes interact with the loop at the end of helix 31 (h31), which contains U1191 (Meyer et al. 2016; Heuer et al. 2017; Ameismeier et al. 2018, 2020; Scaiola et al. 2018). Thus, each of these enzymes should block the binding of the other two and Tsr3 might help order the activities of Rio2 and Rio1 by preventing the rebinding of Rio2 and blocking the premature recruitment of Rio1. To test the first part of this hypothesis, that Tsr3 blocks rebinding of Rio2, we carried out a systematic genetic screen with previously described mutants around h31 that perturb different aspects of 40S head assembly (Supplemental Fig. S3A), looking for mutants that interact genetically with Tsr3 deletion. These mutants were expressed from plasmids encoding either the wild-type or variant protein in the background of yeast strains where the endogenous protein is under a GAL-promoter and depleted by growth in glucose.

Deletion of Tsr3 does not produce a significant growth defect in yeast (Fig. 4A; see also Meyer et al. 2016) or human cells (Babaian et al. 2020). Most of the tested mutants do not show genetic interactions with Tsr3 deletion (Supplemental Fig. S3B and data not shown). In contrast, Rio2_Δloop, Rio2_K105E, Rps20_RK, Rps20_Δloop, Rps15_YRR, and Rps15_RK are all synthetically sick with Tsr3 deletion (Fig. 3A). These mutants block the formation of 80S-like ribosomes at distinct steps (Fig. 3B; Huang et al. 2020) but have two features in common. First, they all surround rRNA h31, which contains U1191, the target of Tsr3 (Fig. 3C). Furthermore, each of these mutants is sensitive to Rio2 overexpression (Fig. 3D; Supplemental Fig. S3C) and impacts Rio2 release (Huang et al. 2020), either directly (Rps15_YRR, Rps15_RK) or indirectly by blocking its phosphorylation, which is required for its release (Rio2_Δloop, Rio2_K105E, Rps20_RK, Rps20_Δloop). Together, these data show that Tsr3 deletion renders cells sensitive to defects in Rio2 release.

The observation that Tsr3 deletion renders cells sensitive to Rio2 release defects was surprising, given that Rio2 is released prior to Tsr3 binding. Nonetheless, these data can be reconciled by a model whereby Tsr3 binding prevents the reassociation of Rio2. To test this hypothesis, we tested the effect of Rio2 overexpression in the presence or absence of Tsr3. Indeed, Rio2 overexpression by the strong TEF promoter (relative to the weaker CYC1 promoter) is detrimental in ΔTsr3 cells, but not in WT cells (Fig. 3E). Moreover, the dominant effect from Rio2 overexpression is rescued by the Rio2 weakly binding variant, Rio2_RQQR (Fig. 3E; Huang et al. 2020). Finally, ΔTsr3 cells phenocopy the cold sensitivity of the Rio2-release-deficient Rio2_D253A mutant (Fig. 3F). Together, these data strongly suggest a role of Tsr3 in preventing the rebinding of Rio2, thereby ensuring its release is irreversible.

To confirm these genetic interactions, which all support a role for Tsr3 in the release of Rio2, we used gradient centrifugation to quantify the binding of Rio2 to nascent 40S ribosomes in cells with or without Tsr3. These data demonstrate that indeed Rio2 accumulates in 80S-like ribosomes when Tsr3 is depleted (Fig. 3G), thus providing strong biochemical support for the genetic data above. In summary, the genetic and biochemical data in this section strongly suggest that Tsr3 binding renders Rio2 dissociation irreversible.

The acp modification activity of Tsr3 is required for its release from nascent 40S subunits

Above, we dissected the timing of Tsr3 function and its potential role in the translation-like cycle by deleting the entire protein. For many rRNA modification enzymes, the presence of protein but not its modification activity is required for ribosome assembly and cell survival (Lafontaine et al. 1995; White et al. 2008; Meyer et al. 2011; Haag et al. 2015;

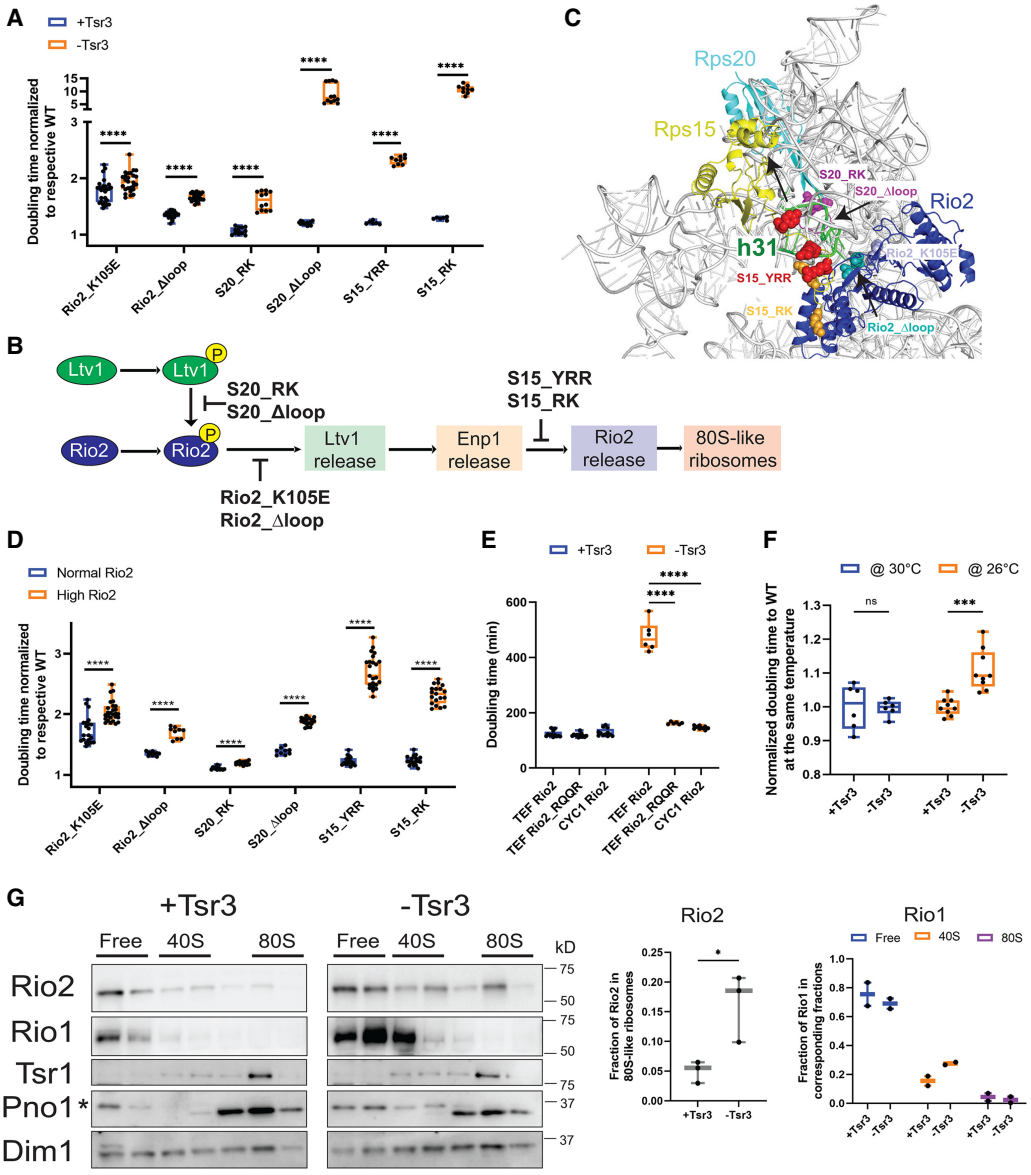

FIGURE 3. Tsr3 ensures that Rio2 release is irreversible. (*A*) Normalized doubling times of yeast cells encoding WT Rio2/Rio2_K105E/Rio2_Δloop, WT S20/S20_RK/S20_Δloop, WT S15/S15_YRR/S15_RK in the presence and absence of Tsr3. WT or mutant proteins were expressed from plasmids in strains where the endogenous protein is under the GAL-promoter and depleted by growth in glucose. Shown in the figure are doubling times of mutants normalized to corresponding WT protein in the same Tsr3 background. Significance was tested using a two-way ANOVA test. (****) $P_{adj} < 0.0001$; $n \geq 6$. (*B*) Scheme showing the order of steps required for the formation of 80S-like ribosomes (Huang et al. 2020) and the effects of the mutants in *A* on these steps. (*C*) A composite structure of yeast pre-40S (PDBID 6FAI) and mature 40S (PDBID 3JAQ) obtained by overlay on Rps18. Mutations in Rio2, Rps15, and Rps20 are highlighted in sphere and colored in the same color as the corresponding text. The loop containing the residues deleted in Rio2_Δloop is unresolved in all structures and the flanking residues, R129 and S145, are highlighted in sphere in cyan. l31 from mature 40S, which is not resolved in pre-40S, is highlighted in green. (*D*) Normalized doubling times of yeast cells encoding WT Rio2/Rio2_K105E/Rio2_Δloop, WT S20/S20_RK/S20_Δloop, WT S15/S15_YRR/S15_RK in the presence of normal levels of Rio2 (expressed under the CYC1 or native promoter) or high levels of Rio2 (expressed under the TEF promoter). WT or mutant proteins were expressed from plasmids in strains where the endogenous protein is under the GAL-promoter and depleted by growth in glucose. Shown in the figure are doubling times of mutants normalized to corresponding WT protein in the same Rio2 background. Significance was tested using a two-way ANOVA test. (****) $P_{adj} < 0.0001$; $n \geq 9$. (*E*) Doubling times of yeast cells encoding Rio2 or Rio2_RQQR expressed from plasmids with the lower expressing CYC1 or the higher expressing TEF promoter in the presence and absence of Tsr3. Significance was tested using a two-way ANOVA test. (****) $P_{adj} < 0.0001$; $n \geq 6$. WT or mutant Rio2 was expressed from plasmids in a strain where the endogenous Rio2 is under the GAL-promoter and depleted by growth in glucose. (*F*) Normalized doubling times of BY4741 (+Tsr3) and ΔTsr3 (−Tsr3) cells grown at 30°C (normal temperature) or 26°C (low temperature), respectively. Significance was tested using a two-way ANOVA test. (***) $P_{adj} < 0.001$; $n \geq 6$. (*G*) (*Left*) Western blots for Rio2, Rio1, Tsr1, Pno1, and Dim1 from gradients in Figure 1C. Asterisk notes the *upper* band corresponding to Pno1. (*Middle*) Quantification of the fraction of Rio2 in 80S-like ribosomes. Significance was tested using an unpaired *t*-test. (*) $P < 0.05$; $n = 3$. (*Right*) Quantification of fraction of Rio1 in free 40S or 80S fractions, respectively. $n = 2$.

Sharma et al. 2015; Zorbas et al. 2015). We therefore made mutations within the active site of Tsr3 to study the role of Tsr3 modification activity in ribosome assembly. We used a previously identified mutant, Tsr3_W114A, which weakens the binding for the substrate, *S*-adenosyl-methionine (SAM), and thus impairs the rRNA modification activity (Meyer et al. 2016). Unexpectedly, abolishing the modification activity of Tsr3 is more detrimental to cell growth than not having Tsr3 (Fig. 4A). Moreover, even expressing inactive Tsr3_W114A in the background of wild-type Tsr3 is detrimental (Fig. 4B). This dominant-negative effect suggests that Tsr3's acp modification activity is required for its release, such that inactive protein would remain stuck on ribosomes, thereby blocking further progression of the assembly cascade. If this is true, we would predict weakly binding variants of Tsr3 to rescue the growth defect of Tsr3_W114A. Indeed, taking advantage of a series of previously identified Tsr3 weakly binding variants designed based on the crystal structure and validated through biochemical assays (Meyer et al. 2016), we observed a significant rescue of the growth defect from Tsr3_W114A when this mutation was combined with any of the tested weak binding mutations (Fig. 4C), further supporting the interpretation that Tsr3 activity is required for its release and that its continued presence blocks a subsequent step(s) in 40S maturation.

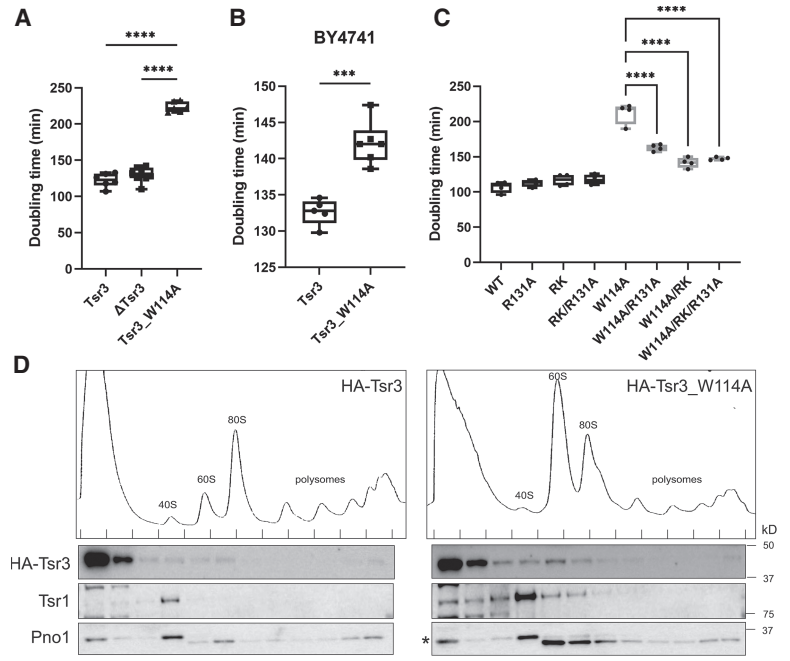

FIGURE 4. The acp modification activity of Tsr3 is required for its release. (*A*) Doubling times of ΔTsr3 cells supplemented with a plasmid encoding WT Tsr3 (Tsr3), an empty vector (ΔTsr3), or a plasmid encoding Tsr3_W114A (Tsr3_W114A). Significance was tested using one-way ANOVA (Sidak's multiple comparisons test). (****) $P_{adj} < 0.0001$; $n \geq 6$. (*B*) Doubling times of BY4741 cells supplemented with plasmids encoding WT Tsr3 or Tsr3_W114A. Significance was tested using an unpaired *t*-test. (***) $P < 0.001$; $n \geq 5$. (*C*) Doubling times of ΔTsr3 cells supplemented with plasmids encoding WT Tsr3 (WT), Tsr3_R131A (R131A), Tsr3_R60A, K65A (RK), Tsr3_ R60A, K65A, R131A (RK/R131A), Tsr3_W114A (W114A), Tsr3_W114A/R131A (W114A/R131A), Tsr3_W114A/R60A, K65A (W114A/RK), or Tsr3_ W114A/R60A, K65A/R131A (W114A/RK/R131A). Significance was tested using one-way ANOVA (Sidak's multiple comparisons test). (****) $P_{adj} < 0.0001$; $n \geq 4$. (*D*) Western blots for HA-tagged Tsr3, Tsr1, and Pno1 from 10% to 50% sucrose gradients from ΔTsr3 cells supplemented with HA-Tsr3 or HA-Tsr3_W114A plasmid. 0.8% formaldehyde was added to the cells when harvesting to stabilize the binding of Tsr3 on ribosomes. Asterisk denotes the *upper* band corresponding to Pno1.

To further test whether the W114A mutation blocks the release of Tsr3 from nascent ribosomes, we probed the accumulation of Tsr3 in ribosomes using sucrose gradient sedimentation. For this purpose, Tsr3 was tagged with an HA tag. As shown in Figure 4D, western analysis of the sucrose gradient samples demonstrates accumulation of Tsr3_W114A in nascent ribosomes. Together, the biochemical and genetic data in this section support a model that Tsr3 activity is required for its release from nascent 40S subunits.

The dissociation of Tsr3 is required to accommodate Rio1 in 80S-like ribosomes

Given that Tsr3 binding is expected to be mutually exclusive not just with Rio2 but also the highly related Rio1, which shares a binding site with Rio2 (Fig. 1A), we hypothesized that the continued presence of Tsr3_W114A blocks the binding of Rio1, leading to the accumulation of 80S-like ribosomes and preventing the release of Nob1 and Pno1 (Parker et al. 2019).

To test whether the Tsr3_W114A mutation leads to the accumulation of 80S-like ribosomes, we used gradient sedimentation to monitor whether the 18S rRNA precursor, 20S rRNA, sediments as 80S-like ribosomes or earlier 40S-sized intermediates when Tsr3 is inactivated (Fig. 5A). These data demonstrate that the Tsr3_W114A mutation results in the accumulation of 80S-like ribosomes (even in the presence of WT Fap7), consistent with Tsr3 blocking the activity of Rio1 (Parker et al. 2019).

To test the second prediction from the model that Tsr3_W114A blocks Rio1 binding, we purified 80S-like ribosomes from cells containing either WT Tsr3 or Tsr3_W114A. 80S-like ribosomes were accumulated by depletion of Fap7 (Strunk et al. 2012) and purified via a TAP-tag on Tsr1 (Ghalei et al. 2017). To our surprise, we find that in the Tsr3_W114A

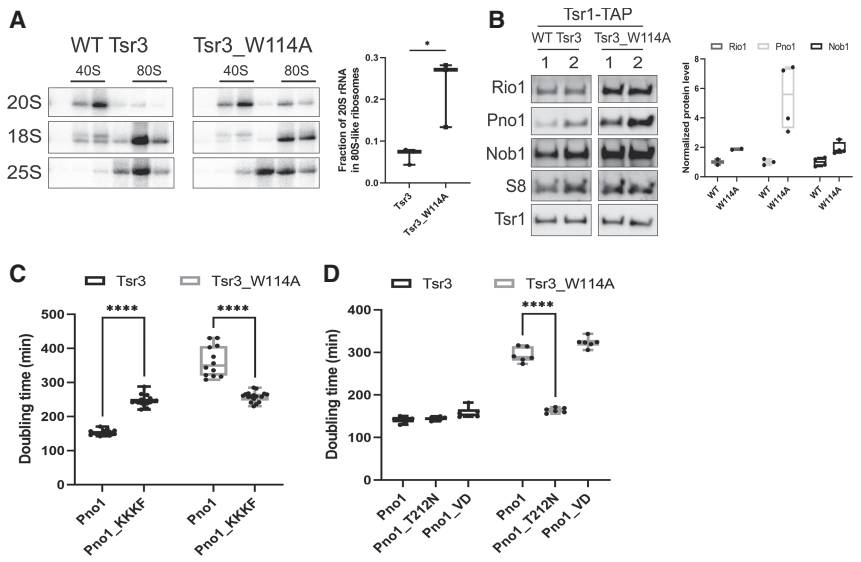

FIGURE 5. The dissociation of Tsr3 is required for Rio1 binding to pre-40S ribosomes. (*A*) Northern blots of 10%–50% sucrose gradients from ΔTsr3 cells expressing plasmid-encoded wild-type (WT) HA-Tsr3 (*left*) or HA-Tsr3_W114A (*middle*) proteins. The positions where 40S and 80S ribosomes sediment are indicated. (*Right*) Quantifications of the data on the *left* indicate the efficiency of formation of 80S-like ribosome formation. Data are shown as mean with standard deviation. Significance was tested using an unpaired *t*-test. (*) $P < 0.05$; $n = 3$. (*B*) (*Left*) 80S-like ribosomes were purified from Tsr1-TAP, ΔTsr3, Gal:Fap7 cells supplemented with HA-Tsr3 or HA-Tsr3_W114A, and probed for bound Rio1, Pno1, Nob1, Rps8 (S8), and Tsr1 from purified pre-40S via Tsr1-TAP from Tsr1-TAP, ΔTsr3, Gal:Fap7 cells supplemented with HA-Tsr3 or HA-Tsr3_W114A. Fap7 were depleted in glucose for more than 16 h. Rio1 signal was normalized to S8 (from the same gel) first before further normalizing Tsr3_W114A to WT Tsr3. Pno1 and Nob1 signal were normalized to Tsr1 first before further normalizing Tsr3_W114A to WT Tsr3. (*Right*) Quantification of normalized Rio1, Pno1, and Nob1 from the *left* and additional replicates. Two biological replicates were tested for each cell. (*C*) Doubling times of ΔTsr3, Gal:Pno1 cells supplemented with WT Tsr3 or Tsr3_W114A and Pno1 or Pno1_KKKF plasmids and grown in glucose. Significance was tested using a two-way ANOVA test. (****) $P_{adj} < 0.0001$; $n \geq 12$. (*D*) Doubling times of ΔTsr3, Gal:Pno1 cells supplemented with WT Tsr3 or Tsr3_W114A and Pno1 or Pno1_T212N or Pno1_VD plasmids and grown in glucose. Significance was tested using a two-way ANOVA test. (****) $P_{adj} < 0.0001$; $n = 6$.

cells Rio1 accumulates on 80S-like ribosomes (Fig. 5B). This finding can be reconciled with the overlap in the Rio1- and Tsr3-binding sites, when considering the observation that Rio1 has two binding sites on nascent 40S subunits. In addition to the functional site shown in Figure 1, a "recruitment site" has also been identified by cryo-EM, which is adjacent to helix 44 (h44) (Ameismeier et al. 2020). We therefore presume that Rio1 is accumulated in this nonfunctional position.

To test this model further, we next asked whether Rio1 is functional in the Tsr3_W114A cells. Rio1 releases Nob1 and Pno1 after 18S rRNA cleavage is complete (Turowski et al. 2014; Belhabich-Baumas et al. 2017; Parker et al. 2019; Ameismeier et al. 2020; Plassart et al. 2021). Thus, if Rio1 was unable to be recruited to its nascent site, we expect Nob1 and Pno1 to accumulate in the 80S-like ribosomes that accumulate in the Tsr3_W114A cells. Indeed, the assembly intermediates that accumulate Rio1 also accumulate Nob1 and Pno1 (Fig. 5B), strongly suggesting that Rio1 is not bound in its functional site adjacent to the platform, but instead at its recruitment site near the A-site.

To further test whether Rio1 was unable to function, we asked whether a previously described suppressor for the deletion of Rio1, Pno1_KKKF (K208E/K211E/K213E/F214A) (Parker et al. 2019), can rescue the growth defects observed from the Tsr3_W114A mutation. This mutation leads to weak binding of Pno1, thereby bypassing the need for Rio1 to release Pno1, and its binding partner Nob1 (Johnson et al. 2017; Parker et al. 2019). As before, wild-type Pno1 or Pno1 variants were expressed from plasmids in a yeast strain, grown in glucose, where endogenous Pno1 is under GAL-inducible control. Indeed, Pno1_KKKF largely rescues the growth defect of the Tsr3_W114A mutation, even though it leads to slow growth by itself (Fig. 5C). This observation provides strong support for the model that Tsr3 binding blocks the recruitment of Rio1 into its functional site.

To further validate this suggestion, we tested whether other mutants that bypass Rio1 can rescue Tsr3_W114A. After mapping Pno1 mutations found in cancer cells (Cerami et al. 2012; Gao et al. 2013) (www.cbioportal.org) onto the Pno1 structure (Supplemental Fig. S4A), we focused on two mutants. Pno1_T212N is located adjacent to Pno1_KKKF and should thus similarly weaken Pno1 binding, while Pno1_VD (V225A/D228N) appears to affect Pno1's structure and should thus not affect its binding to ribosomes. Sucrose gradient sedimentation experiments demonstrate that, as expected, Pno1_T212N is bound weakly to pre-40S ribosomes, resulting in reduced cosedimentation with ribosomes and accumulation on top of the gradient (Supplemental Fig. S4C). In contrast, Pno1_VD is not weakly bound. Moreover, Pno1_T212N, but not Pno1_VD, rescues the growth defect from Rio1 depletion (Supplemental Fig. S4B), as previously shown for Pno1_KKKF (Parker et al. 2019). Thus, Pno1_KKKF and Pno1_T212N bind pre-40S weakly and rescue the growth defect from Rio1 depletion, apparently because they are self-releasing. In contrast, Pno1_VD is not self-releasing and therefore cannot rescue Rio1 depletion.

Next, we asked whether the cancer-associated Pno1_T212N also rescues the growth defect from the

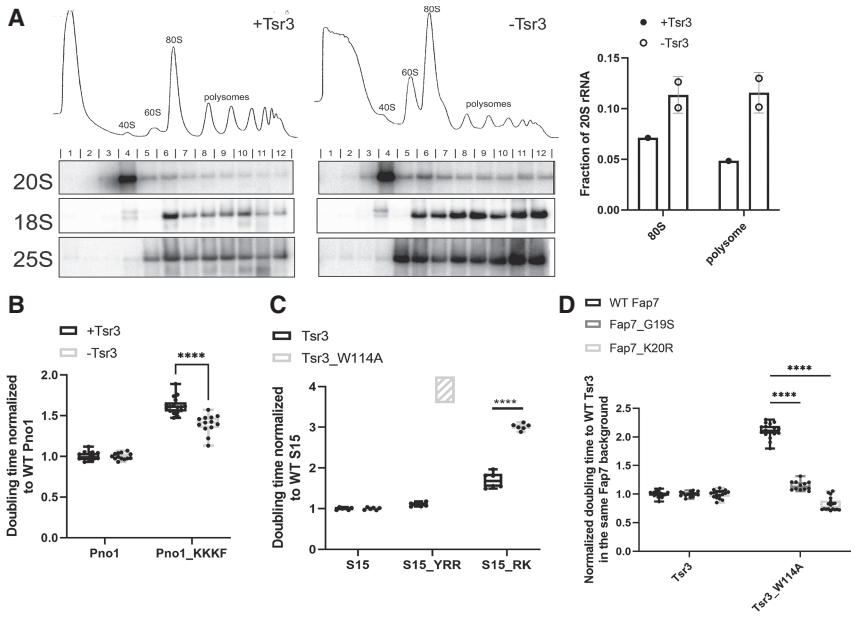

FIGURE 6. Tsr3 establishes the hierarchy of Rio kinase function. (*A*) 10%–50% sucrose gradients of lysates from cells of WT BY4741 (+Tsr3, *left*) or ΔTsr3 (−Tsr3, *middle*). Shown below the absorbance profiles at 254 nm are northern blots of 20S, 18S, and 25S rRNA. (*Right*) Quantifications of the data on the *left*. Fraction of 20S rRNA in 80S (fraction 6–7) and polysome (fraction 8–12) are quantified. $n = 2$. (*B*) Normalized doubling times of ΔTsr3, Gal:Pno1 cells supplemented with WT Tsr3 or empty vector and Pno1 or Pno1_KKKF plasmids and grown in glucose. Significance was tested using a two-way ANOVA test. (****) $P_{adj} < 0.0001$; $n \geq 13$. (*C*) Normalized doubling times of ΔTsr3, Gal:Rps15 cells supplemented with WT Tsr3 or Tsr3_W114A and WT Rps15 or Rps15_YRR or Rps15_RK plasmids and grown in glucose. Cells with Tsr3_W114A and Rps15_YRR plasmids do not grow and are therefore shown as a box filled with diagonal lines. Significance was tested using a two-way ANOVA test. (****) $P_{adj} < 0.0001$; $n = 6$. (*D*) Normalized doubling times of ΔTsr3, Gal:Fap7 cells supplemented with WT Tsr3 or Tsr3_W114A and WT Fap7 or Fap7_G19S or Fap7_K20R plasmids and grown in glucose. Significance was tested using a two-way ANOVA test. (****) $P_{adj} < 0.0001$; $n \geq 15$.

Tsr3_W114A mutation as expected if this mutation blocks Rio1 binding. Indeed, Pno1_T212N can rescue the growth defects from the Tsr3_W114A mutation (Fig. 5D). Importantly, this effect is observed only from the self-releasing Pno1_KKKF and Pno1_T212N mutations but not Pno1_VD, demonstrating that it is not a general feature of Pno1 mutants but requires the weak binding of Pno1. Together, these biochemical and genetic data strongly suggest that release of Tsr3 is required for the binding of Rio1 to its functional state near the platform, and that in mutants that block Tsr3 release, Rio1 accumulates on nascent 40S in a nonfunctional position, likely corresponding to the previously described position adjacent to h44 (Ameismeier et al. 2020).

Tsr3 establishes the hierarchy of Rio kinase activity in 40S ribosome assembly

Above, we have provided evidence that the inactivation of Tsr3 impairs its release, and that the resulting persistence of Tsr3 blocks Rio1 binding. This observation suggests that the release of Tsr3 helps to temporally regulate Rio1. If this hypothesis is correct, then we predict ΔTsr3 cells to bind Rio1 prematurely. To test this prediction, we probed the binding of Rio1 to nascent 40S subunits using sucrose gradient centrifugation from cells stalled prior to the Fap7-dependent step by Fap7 depletion (Fig. 3G). These data show that there is an increase of Rio1 bound to 40S-sized pre-40S subunits, as expected if in the absence of Tsr3, Rio1 binds once Rio2 has dissociated and even prior to the formation of 80S-like ribosomes. Because Rio1 normally binds to 80S-like ribosomes after the Fap7-dependent step, this observation provides evidence for premature binding of Rio1 in the absence of Tsr3. To further confirm these data, we probed for a trace of premature Rio1 activity, we have previously described. Release of immature 20S rRNA into the polysomes requires the Rio1-mediated dissociation of Nob1, establishing Nob1/Rio1 as gatekeepers for ensuring only mature 18S rRNA-containing ribosomes translate mRNA into protein (Parker et al. 2019). Thus, 20S pre-rRNA in the polysomes is a sign of misregulated, premature Rio1 activity (or genetically weakened Nob1 binding, which bypasses Rio1 entirely). Indeed, we observed a more than twofold increase of 20S in polysomes in Tsr3 deletion cells (Fig. 6A), providing strong support for premature Rio1 activity in ΔTsr3 cells.

To further confirm this model, we tested for genetic interactions between Tsr3 deletion and Rio1-independent Nob1 release, via the previously characterized Pno1_KKKF mutant, which also leads to 20S escaping into polysomes. If Tsr3 deletion leads to premature Rio1 activity, then we predict that it has no (or a reduced) effect in cells where Rio1 is not required for 20S rRNA release into the polysomes. Indeed, this predicted epistasis between ΔTsr3 and Pno1_KKKF is exactly what we observe (Fig. 6B), providing additional genetic evidence to support the above biochemical data that Tsr3 deletion leads to premature Rio1-dependent release of Nob1. Together, these data demonstrate the importance of Tsr3-mediated temporal regulation of Rio1 binding for faithful 40S maturation.

To test whether Tsr3's presence was enough to establish the hierarchy in Rio kinase activity, or whether its activity was required for this function, we asked whether the Tsr3_W114A mutant interacted genetically with the Rio2-

release-deficient mutants. If the role for Tsr3 was simply in competition with Rio2, then we would expect Tsr3_W114A to efficiently compete against Rio2. In this model, the Tsr3_W114A mutant should not show genetic interactions with the Rio2-release-deficient Rps15_RK or Rps15_YRR mutants. In contrast, if the ability to modify the RNA is important, then we expect the Tsr3_W114A mutant to be synthetically sick with the Rio2-release- defective Rps15_YRR and Rps15_RK, as we observe for the Tsr3 deletion strain. Indeed, we observe that Tsr3_W114A is synthetically sick with the Rio2-release-defective Rps15_YRR and Rps15_RK (Fig. 6C). This synthetic interaction does not simply arise because the intermediate able to bind Rio1 is depleted, as depletion of this intermediate by Fap7 inactivation leads to epistasis, not negative genetic interactions (Fig. 6D).

DISCUSSION

Tsr3 coordinates Rio2 and Rio1 kinase binding and provides directionality to late stages of 40S maturation

Rio2 and Rio1 are two highly homologous kinases, which bind subsequent to each other to the same site on the head of the nascent small ribosomal subunit (Fig. 1A). While there, Rio2 ensures that l31 of 18S rRNA remains unfolded, thereby chaperoning rRNA folding of the nearby junction between helices 34, 35, and 38 (Huang and Karbstein 2021), while Rio1 releases the nuclease Nob1 and its interaction partner Pno1 after rRNA maturation is complete, thus allowing the newly made subunit to start translation (Parker et al. 2019). How cells ensure that Rio1 functions after Rio2 and not before, which would release Nob1 from immature ribosomes and enable them to start translation, remains unclear.

Here we show that the conserved rRNA-modifying enzyme Tsr3 uses its modification activity to separate and temporally organize the activities of Rio2 and Rio1, thereby ensuring that their functional order is maintained and only correctly folded and fully matured ribosomes are released into the translating pool (Fig. 7).

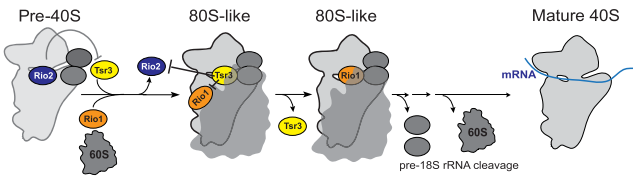

FIGURE 7. Tsr3 coordinates the activity of Rio1 and Rio2. Schematic model showing how Tsr3 coordinates and separates the activities of Rio2 and Rio1. Rio2 binding to pre-40S blocks premature binding of Tsr3. Once bound though, Tsr3 blocks rebinding of Rio2 as well as premature binding of Rio1 at its functional site. Its initial recruitment adjacent to h44 is unaffected by Tsr3 binding.

Specifically, our data show that Tsr3, which shares a binding site with Rio2 and Rio1, functions within 80S-like ribosomes and thus after Rio2 is released but before Rio1 binds. Moreover, the data also indicate that Tsr3 renders Rio2 dissociation irreversible. In addition, we show that modification activity is required to release Tsr3, and that blocking Tsr3 release blocks the binding of Rio1 to its functional site near the platform. Thus, together, these data show that Tsr3 separates the activities of Rio2 and Rio1. The importance of this role for Tsr3 in establishing the hierarchy of binding of these two proteins is demonstrated by the observation that cells lacking Tsr3 release immature subunits into the translating pool as expected from premature activity of Rio1.

The ability to modify rRNA is required for Tsr3's function in ordering Rio activity

How does Tsr3 order Rio2 and Rio1 activity, and thereby impart directionality to the process? Tsr3 uses *S*-adenosylmethionine (SAM) as a donor for the amino-carboxy-propyl-(acp) group that is transferred onto U1191 (Meyer et al. 2016), leaving behind methylthioadenosine (MTA). Because SAM is produced using ATP, Tsr3 essentially consumes energy in the form of ATP. Thus, it is possible that Tsr3 might simply use the energy from SAM/ATP to provide directionality. In this model, SAM-bound Tsr3 might effectively compete with both Rio2 and Rio1, while the MTA-bound Tsr3 can no longer compete with Rio1, perhaps due to some conformational differences. Additionally, or alternatively, it is also possible that the modification itself contributes to the discrimination. Indeed, our genetic data support a role for Tsr3 that goes beyond simply being a competitor and indicate that its modification activity is required for establishing Rio kinase hierarchy.

Energy-driven changes in AF-binding sites provide directionality to the process

As described above, there are numerous instances during ribosome assembly where two or more assembly factors bind the same location successively, as we have shown here for Rio2 and Rio1. Examples during small subunit assembly include snR35 and Emg1, which bind the same rRNA loop as Rio2, Tsr3, and Rio1 during the early, nucleolar stages of 40S assembly (Fig. 1B). Similarly, the assembly factor Pno1 replaces Krr1 on the nascent platform (Sturm et al. 2017), only to be replaced with Rps26 in the final maturation step (Strunk et al. 2012; Ferretti et al. 2017; Parker et al. 2019). Moreover, Tsr1 replaces Bms1 on the nascent body (Gelperin et al. 2001; Strunk et al. 2011; Kornprobst et al. 2016; McCaughan et al. 2016). Examples during 60S maturation include Nog1, Rei1, and Reh1 binding the peptide exit channel (Kallstrom et al. 2003; Hung and Johnson 2006; Lebreton et al. 2006; Fuentes et al. 2007; Parnell

and Bass 2009; Greber et al. 2016; Wu et al. 2016; Ma et al. 2017; Klingauf-Nerurkar et al. 2020) and Mrt4, Yvh1, and Rpp0 binding the nascent P-stalk (Kemmler et al. 2009; Lo et al. 2009). Some of these factors may also use energy for their ordered activity (Bms1 and Nog1 are GTPases and Yvh1 is annotated as a phosphatase; see also Fig. 1B), but that is not universally true. Nonetheless, in all cases, the environment of the assembly factors changes in going from the early to the late-binding factors. For example, Tsr1 interacts with the decoding site helix, h44, while Bms1 blocks h44 incorporation into the subunit (or is blocked by its presence). In addition to being blocked by Bms1, h44 is held away by interactions with the early-binding assembly factors Utp12/Utp13 and Utp22, which appear to dissociate after maturation of the 5′-end of 18S rRNA. Thus, once the 5′-end of 18S rRNA is matured and h44 is incorporated in its native position, Bms1 will no longer be able to bind.

Similarly, while both Krr1 and Pno1 are bound very similarly to h23 and Rps14, Krr1 is also bound to Faf1, which in turn binds to the 5′-ETS helix H6. Thus, early in transcription of rRNA, Faf1 is recruited via binding to the 5′-ETS, and then can recruit Krr1, over Pno1. During assembly, H6 is degraded, while formation of h24 and h45, which is stabilized by the recruitment of Dim1, excludes Krr1 via steric contacts. In contrast, Pno1 is stabilized by an interaction with h45. Thus, the temporal ordering of Krr1 and Pno1 (or Bms1/Tsr1) binding is achieved by changes in the rRNA-binding site, akin to the Tsr3-dependent changes in the Rio-binding site. Notably the differences are that in the case of Krr1/Pno1 and Bms1/Tsr1, the changes arise from rRNA folding and maturation, while in the Rio case, the changes arise from a covalent modification. This might be necessary because the subunits are so far matured that few (and small) changes in folding or processing are left to impose order.

Other modification enzymes also require their activity for release

Making the release of Tsr3 and subsequent 40S maturation steps dependent on the completion of its modification reaction ensures that most, if not all, subunits are modified. Interestingly, Tsr3 is not the only rRNA modification enzyme whose release appears to require enzymatic activity. Rrp8 and Bmt2, which methylate the N1 of A645 and A2142 in 25S rRNA, respectively, both appear to have the same property (Peifer et al. 2012; Sharma et al. 2013). Both of these enzymes are nonessential and, like Tsr3, do not demonstrate any phenotype upon their deletion (at 30°C). In contrast, nonfunctional mutants of Rrp8 and Bmt2 both lead to the accumulation of half-mer ribosomes, indicative of defects in 60S maturation (Peifer et al. 2012; Sharma et al. 2018). Like Tsr3, Rrp8 functions after snoRNA mediated rRNA modification at A649/650. Intriguingly, A649 is involved in a highly unusual RNA structure, which sets up the back end of the large subunit's P- and A-sites, again similar to Tsr3, whose target site forms the small subunit's P-site. Furthermore, for the bacterial homolog of Dim1, KsgA, it has also been reported that its activity is required for its release, leading to strong dominant-negative effects from an inactive mutant (Connolly et al. 2008). Dim1 modifies residues in the small subunit's P-site. These defects are not observed in the yeast system (Pulicherla et al. 2009), presumably because in yeast Dim1 is actively released via the ATPase Fap7 (Ghalei et al. 2017). Thus, it appears likely that Tsr3 and Rrp8 (and bacterial KsgA) might have evolved to ensure a high modification rate in the functional centers of the ribosome.

What function does the modification of Tsr3 serve? As described above, the Tsr3 modification site forms part of the small subunit's P-site. Yet, deletion of Tsr3 in yeast provides a <10% defect in growth, and no obvious defect in global translation. Similarly, Tsr3 deletion in human cells does not produce growth or global translation defects (Babaian et al. 2020). Nonetheless, a very small subset of mRNAs (<20) displays statistically significant changes in translational efficiency, although not enough to change the proteome. However, what is unique about these mRNAs, and thus causes the sensitivity to the absence of the modification, remains to be seen. Of note, many cancer cells are characterized by reduced levels of the modification (Babaian et al. 2020), supporting its importance for ribosome assembly and/or function. Interestingly, for snR35 and Emg1, the first two factors in the U1191 modification cascade, we have recently reported roles in rRNA folding (Huang and Karbstein 2021). While this does not preclude additional roles for the modifications in functionality downstream, these findings should at least lead us to think about roles for rRNA modification enzymes that go beyond the modification and include ensuring efficient and faithful assembly of the subunit.

MATERIALS AND METHODS

Plasmids and yeast strains

Yeast strains (Supplemental Table S1) were obtained from Yeast Knockout Collection (Horizon) or generated by standard homologous recombination (Longtine et al. 1998), and confirmed by PCR, serial dilution, and western blotting if antibodies were available. Plasmids (Supplemental Table S2) were constructed using standard cloning techniques and confirmed via Sanger sequencing.

Growth curve measurements

Freshly transformed cells were grown in YPD or glucose minimal media (if the supplemented plasmid is not essential) overnight, and then diluted into fresh YPD for 3–6 h before inoculating into 96-well plates (Thermo Fisher Scientific) at a starting OD600 between 0.04 and 0.1. A Synergy 2 plate reader

(BioTek) was used to record the OD600 for 48 h, while shaking at 30°C. Doubling times were calculated using data points within the mid-log phase using GraphPad Prism 9. Data were averaged from at least six biological replicates of three different colonies and two independent measurements. For all the growth curve assays, detailed yeast strains and plasmids used in each study were summarized in Supplemental Table S3. Statistical analyses for each measurement are detailed in the respective figure legend.

Serial dilution

Overnight cultured cells were spotted on glucose or galactose dropout plates with 10-fold serial dilutions. The size of single colonies is used to assess cell growth.

Primer extension assay for acp modification

Different pre-40S intermediates were purified using TAP-tagged proteins via IgG beads as previously described (Parker et al. 2019; Huang and Karbstein 2021). Mature 40S were purified via Rps3-TAP. rRNAs from pre-40S intermediates were phenol chloroform extracted and further cleaned using RNeasy Mini Columns (Qiagen). A total of 1 µg of rRNA was used for each reverse transcription reaction using a primer that starts at 1241 of 18S rRNA (sequence listed in Supplemental Table S4). rRNA was annealed with radioactively labeled primer before reverse transcription with SuperScript III (Thermo Fisher Scientific) at 50°C for 10 min. rRNAs were then hydrolyzed by addition of 200 mM NaOH at 95°C for 5 min. cDNAs were separated by 8% TBE-urea gels and visualized by Typhoon FLA 9000 (GE Healthcare). Sequencing ladders were made using the Sequenase 2.0 DNA Sequencing Kit (Thermo Fisher Scientific) and the same primer as above and 35S rDNA plasmid as template. As previously described (Meyer et al. 2016), acp modification causes a prominent stop during reverse transcription, which we validated by the sequencing ladders and the missing stop signal in ribosomes from ΔTsr3 yeast. When assaying mature ribosomes, primer extensions were carried out using total RNA from respective cells. Total RNAs was isolated using the hot phenol method and cleaned by an RNeasy Mini Column.

In vivo subunit joining assay

Gal:Fap7 strains in combination with the additional mutation of interest were grown to mid-log phase in galactose before inoculating into YPD for at least 16 h to deplete Fap7 and accumulate 80S-like ribosomes. Formation of 80S-like ribosomes was assayed by sucrose gradient fractionation and northern blotting as previously described (Strunk et al. 2012; Huang et al. 2020), and the fraction of 20S rRNA in 80S-like ribosomes quantified. Oligos used for northern analysis are listed in Supplemental Table S4. At least two biological replicates were assayed for each mutant.

Stabilization of the binding of Tsr3 on ribosomes via in vivo cross-linking

Formaldehyde cross-linking was conducted as previously described (Valášek et al. 2007). Briefly, 200 ml of cells grown to mid-log phase in minimal media were first cooled by adding 50 g crushed ice per 200 ml of culture, before adding formaldehyde to a final concentration of 0.8%. The reaction was incubated on ice for 1 h and stopped by addition of glycine to a final concentration of 0.1 M. Cells were pelleted through centrifugation and resuspended in gradient lysis buffer (20 mM HEPES pH 7.4, 5 mM $MgCl_2$, 100 mM KCl, 1 mM benzamidine, 1 mM PMSF, protease inhibitor tablet, leupeptin, aprotinin, pepstatin, 2 mM DTT) before flash freezing in liquid N_2. Cleared cell lysates were applied on 10%–50% sucrose gradients and the distribution of Tsr3 and other assembly factors were probed from each fraction of the gradients using western blotting as previously described (Strunk et al. 2012; Huang et al. 2020).

TAP purification of different 40S intermediates

Different pre-40S intermediates were purified using TAP-tagged proteins via IgG beads as previously described (Parker et al. 2019; Huang and Karbstein 2021). Briefly, 2–3 liters of cells were harvested in mid-log phase and lysed in IgG-binding buffer (50 mM Tris pH 7.5, 100 mM NaCl, 10 mM $MgCl_2$, 0.075% NP40). Cleared lysates were incubated with IgG beads (PHARMACIA 17-0969-01) at 4°C for 2 h. After flow through and wash steps, 1 : 100 TEV protease (Invitrogen) was added and incubated with the beads at 16°C for 2 h in elution buffer (IgG binding buffer + 0.5 mM EDTA + 2 mM DTT) before elution. The elution products were subject to RNA extraction or acetone precipitation for primer extension or western blots, respectively.

Quantification and statistical analysis

Northern blots were visualized with a Typhoon FLA 9000 (GE Healthcare). Quantity One (Bio-Rad) was used to analyze northern blot results. Western blot images were taken by imager ChemiDoc MP Imaging System from Bio-Rad after applying luminescence substrates (Bio-Rad). Image Lab (Bio-Rad) was used to analyze western blot results. Statistical analyses were performed using GraphPad Prism version 9 (GraphPad Software, San Diego, California). Statistical tests were used as indicated in the respective figure legends.

SUPPLEMENTAL MATERIAL

Supplemental material is available for this article.

ACKNOWLEDGMENTS

We thank members of the Karbstein laboratory for discussion and comments on the manuscript. This work was supported by National Institutes of Health (NIH) grant R35-GM136323, and Howard Hughes Medical Institute (HHMI) Faculty Scholar grant 55108536 to K.K., and a Farris Foundation fellowship to H.H.

Received September 28, 2021; accepted December 28, 2021.

REFERENCES

Ameismeier M, Cheng J, Berninghausen O, Beckmann R. 2018. Visualizing late states of human 40S ribosomal subunit maturation. *Nature* **558:** 249–253. doi:10.1038/s41586-018-0193-0

Ameismeier M, Zemp I, van den Heuvel J, Thoms M, Berninghausen O, Kutay U, Beckmann R. 2020. Structural basis for the final steps of human 40S ribosome maturation. *Nature* **587:** 683–687. doi:10.1038/s41586-020-2929-x

Babaian A, Rothe K, Girodat D, Minia I, Djondovic S, Milek M, Spencer Miko SE, Wieden HJ, Landthaler M, Morin GB, et al. 2020. Loss of $m^1acp^3\psi$ ribosomal RNA modification is a major feature of cancer. *Cell Rep* **31:** 107611. doi:10.1016/j.celrep.2020.107611

Bassler J, Hurt E. 2019. Eukaryotic ribosome assembly. *Annu Rev Biochem* **88:** 281–306. doi:10.1146/annurev-biochem-013118-110817

Belhabich-Baumas K, Joret C, Jády BE, Plisson-Chastang C, Shayan R, Klopp C, Henras AK, Henry Y, Mougin A. 2017. The Rio1p ATPase hinders premature entry into translation of late pre-40S pre-ribosomal particles. *Nucleic Acids Res* **45:** 10824–10836. doi:10.1093/nar/gkx734

Breker M, Gymrek M, Schuldiner M. 2013. A novel single-cell screening platform reveals proteome plasticity during yeast stress responses. *J Cell Biol* **200:** 839–850. doi:10.1083/jcb.201301120

Breker M, Gymrek M, Moldavski O, Schuldiner M. 2014. LoQAtE—localization and quantitation ATlas of the yeast proteomE. A new tool for multiparametric dissection of single-protein behavior in response to biological perturbations in yeast. *Nucleic Acids Res* **42:** D726–D730. doi:10.1093/nar/gkt933

Cerami E, Gao J, Dogrusoz U, Gross BE, Sumer SO, Aksoy BA, Jacobsen A, Byrne CJ, Heuer ML, Larsson E, et al. 2012. The cBio cancer genomics portal: an open platform for exploring multidimensional cancer genomics data. *Cancer Discov* **2:** 401–404. doi:10.1158/2159-8290.cd-12-0095

Chaker-Margot M. 2018. Assembly of the small ribosomal subunit in yeast: mechanism and regulation. *RNA* **24:** 881–891. doi:10.1261/rna.066985.118

Cheng J, Bassler J, Fischer P, Lau B, Kellner N, Kunze R, Griesel S, Kallas M, Berninghausen O, Strauss D, et al. 2019. Thermophile 90S pre-ribosome structures reveal the reverse order of co-transcriptional 18S rRNA subdomain integration. *Mol Cell* **75:** 1256–1269.e1257. doi:10.1016/j.molcel.2019.06.032

Cheng J, Lau B, La Venuta G, Ameismeier M, Berninghausen O, Hurt E, Beckmann R. 2020. 90S pre-ribosome transformation into the primordial 40S subunit. *Science* **369:** 1470–1476. doi:10.1126/science.abb4119

Connolly K, Rife JP, Culver G. 2008. Mechanistic insight into the ribosome biogenesis functions of the ancient protein KsgA. *Mol Microbiol* **70:** 1062–1075. doi:10.1111/j.1365-2958.2008.06485.x

Davis JH, Tan YZ, Carragher B, Potter CS, Lyumkis D, Williamson JR. 2016. Modular assembly of the bacterial large ribosomal subunit. *Cell* **167:** 1610. doi:10.1016/j.cell.2016.11.020

de la Cruz J, Karbstein K, Woolford JL Jr. 2015. Functions of ribosomal proteins in assembly of eukaryotic ribosomes in vivo. *Annu Rev Biochem* **84:** 93–129. doi:10.1146/annurev-biochem-060614-033917

Du Y, An W, Zhu X, Sun Q, Qi J, Ye K. 2020. Cryo-EM structure of 90S small ribosomal subunit precursors in transition states. *Science* **369:** 1477–1481. doi:10.1126/science.aba9690

Ferreira-Cerca S, Sagar V, Schafer T, Diop M, Wesseling AM, Lu HY, Chai E, Hurt E, LaRonde-LeBlanc N. 2012. ATPase-dependent role of the atypical kinase Rio2 on the evolving pre-40S ribosomal subunit. *Nat Struct Mol Biol* **19:** 1316. doi:10.1038/nsmb.2403

Ferretti MB, Ghalei H, Ward EA, Potts EL, Karbstein K. 2017. Rps26 directs mRNA-specific translation by recognition of Kozak sequence elements. *Nat Struct Mol Biol* **24:** 700–707. doi:10.1038/nsmb.3442

Fuentes JL, Datta K, Sullivan SM, Walker A, Maddock JR. 2007. In vivo functional characterization of the *Saccharomyces cerevisiae* 60S biogenesis GTPase Nog1. *Mol Genet Genomics* **278:** 105–123. doi:10.1007/s00438-007-0233-1

Gao J, Aksoy BA, Dogrusoz U, Dresdner G, Gross B, Sumer SO, Sun Y, Jacobsen A, Sinha R, Larsson E, et al. 2013. Integrative analysis of complex cancer genomics and clinical profiles using the cBioPortal. *Sci Signal* **6:** pl1. doi:10.1126/scisignal.2004088

Geerlings TH, Faber AW, Bister MD, Vos JC, Raue HA. 2003. Rio2p, an evolutionarily conserved, low abundant protein kinase essential for processing of 20 S pre-rRNA in *Saccharomyces cerevisiae*. *J Biol Chem* **278:** 22537–22545. doi:10.1074/jbc.M300759200

Gelperin D, Horton L, Beckman J, Hensold J, Lemmon SK. 2001. Bms1p, a novel GTP-binding protein, and the related Tsr1p are required for distinct steps of 40S ribosome biogenesis in yeast. *RNA* **7:** 1268–1283. doi:10.1017/S1355838201013073

Ghalei H, Schaub FX, Doherty JR, Noguchi Y, Roush WR, Cleveland JL, Stroupe ME, Karbstein K. 2015. Hrr25/CK1δ-directed release of Ltv1 from pre-40S ribosomes is necessary for ribosome assembly and cell growth. *J Cell Biol* **208:** 745–759. doi:10.1083/jcb.201409056

Ghalei H, Trepreau J, Collins JC, Bhaskaran H, Strunk BS, Karbstein K. 2017. The ATPase Fap7 tests the ability to carry out translocation-like conformational changes and releases Dim1 during 40S ribosome maturation. *Mol Cell* **67:** 990–1000.e1003. doi:10.1016/j.molcel.2017.08.007

Greber BJ, Gerhardy S, Leitner A, Leibundgut M, Salem M, Boehringer D, Leulliot N, Aebersold R, Panse VG, Ban N. 2016. Insertion of the biogenesis factor rei1 probes the ribosomal tunnel during 60S maturation. *Cell* **164:** 91–102. doi:10.1016/j.cell.2015.11.027

Haag S, Kretschmer J, Bohnsack MT. 2015. WBSCR22/Merm1 is required for late nuclear pre-ribosomal RNA processing and mediates N^7-methylation of G1639 in human 18S rRNA. *RNA* **21:** 180–187. doi:10.1261/rna.047910.114

Hector RD, Burlacu E, Aitken S, Le Bihan T, Tuijtel M, Zaplatina A, Cook AG, Granneman S. 2014. Snapshots of pre-rRNA structural flexibility reveal eukaryotic 40S assembly dynamics at nucleotide resolution. *Nucleic Acids Res* **42:** 12138–12154. doi:10.1093/nar/gku815

Heuer A, Thomson E, Schmidt C, Berninghausen O, Becker T, Hurt E, Beckmann R. 2017. Cryo-EM structure of a late pre-40S ribosomal subunit from *Saccharomyces cerevisiae*. *Elife* **6:** e30189. doi:10.7554/eLife.30189

Huang H, Karbstein K. 2021. Assembly factors chaperone ribosomal RNA folding by isolating helical junctions that are prone to misfolding. *Proc Natl Acad Sci* **118:** e2101164118. doi:10.1073/pnas.2101164118

Huang H, Ghalei H, Karbstein K. 2020. Quality control of 40S ribosome head assembly ensures scanning competence. *J Cell Biol* **219:** e202004161. doi:10.1083/jcb.202004161

Hung NJ, Johnson AW. 2006. Nuclear recycling of the pre-60S ribosomal subunit-associated factor Arx1 depends on Rei1 in *Saccharomyces cerevisiae*. *Mol Cell Biol* **26:** 3718–3727. doi:10.1128/mcb.26.10.3718-3727.2006

Johnson MC, Ghalei H, Doxtader KA, Karbstein K, Stroupe ME. 2017. Structural heterogeneity in pre-40S ribosomes. *Structure* **25:** 329–340. doi:10.1016/j.str.2016.12.011

Kallstrom G, Hedges J, Johnson A. 2003. The putative GTPases Nog1p and Lsg1p are required for 60S ribosomal subunit biogenesis and are localized to the nucleus and cytoplasm, respectively. *Mol Cell Biol* **23:** 4344–4355. doi:10.1128/mcb.23.12.4344-4355.2003

Kemmler S, Occhipinti L, Veisu M, Panse VG. 2009. Yvh1 is required for a late maturation step in the 60S biogenesis pathway. *J Cell Biol* **186:** 863–880. doi:10.1083/jcb.200904111

Klingauf-Nerurkar P, Gillet LC, Portugal-Calisto D, Oborska-Oplova M, Jager M, Schubert OT, Pisano A, Pena C, Rao S, Altvater M, et al. 2020. The GTPase Nog1 co-ordinates the assembly, maturation and quality control of distant ribosomal functional centers. *Elife* **9:** e52474. doi:10.7554/eLife.52474

Klinge S, Woolford JL. 2019. Ribosome assembly coming into focus. *Nat Rev Mol Cell Biol* **20:** 116–131. doi:10.1038/s41580-018-0078-y

Knuppel R, Christensen RH, Gray FC, Esser D, Strauss D, Medenbach J, Siebers B, MacNeill SA, LaRonde N, Ferreira-Cerca S. 2018. Insights into the evolutionary conserved regulation of Rio ATPase activity. *Nucleic Acids Res* **46:** 1441–1456. doi:10.1093/nar/gkx1236

Kornprobst M, Turk M, Kellner N, Cheng J, Flemming D, Kos-Braun I, Kos M, Thoms M, Berninghausen O, Beckmann R, et al. 2016. Architecture of the 90S pre-ribosome: a structural view on the birth of the eukaryotic ribosome. *Cell* **166:** 380–393. doi:10.1016/j.cell.2016.06.014

Lafontaine D, Vandenhaute J, Tollervey D. 1995. The 18S rRNA dimethylase Dim1p is required for pre-ribosomal RNA processing in yeast. *Genes Dev* **9:** 2470–2481. doi:10.1101/gad.9.20.2470

Lebaron S, Schneider C, van Nues RW, Swiatkowska A, Walsh D, Bottcher B, Granneman S, Watkins NJ, Tollervey D. 2012. Proofreading of pre-40S ribosome maturation by a translation initiation factor and 60S subunits. *Nat Struct Mol Biol* **19:** 744–753. doi:10.1038/nsmb.2308

Lebreton A, Saveanu C, Decourty L, Rain JC, Jacquier A, Fromont-Racine M. 2006. A functional network involved in the recycling of nucleocytoplasmic pre-60S factors. *J Cell Biol* **173:** 349–360. doi:10.1083/jcb.200510080

Liang XH, Liu Q, Fournier MJ. 2009. Loss of rRNA modifications in the decoding center of the ribosome impairs translation and strongly delays pre-rRNA processing. *RNA* **15:** 1716–1728. doi:10.1261/rna.1724409

Lo KY, Li Z, Wang F, Marcotte EM, Johnson AW. 2009. Ribosome stalk assembly requires the dual-specificity phosphatase Yvh1 for the exchange of Mrt4 with P0. *J Cell Biol* **186:** 849–862. doi:10.1083/jcb.200904110

Longtine MS, McKenzie A III, Demarini DJ, Shah NG, Wach A, Brachat A, Philippsen P, Pringle JR. 1998. Additional modules for versatile and economical PCR-based gene deletion and modification in *Saccharomyces cerevisiae*. *Yeast* **14:** 953–961. doi:10.1002/(SICI)1097-0061(199807)14:10<953::AID-YEA293>3.0.CO;2-U

Ma C, Wu S, Li N, Chen Y, Yan K, Li Z, Zheng L, Lei J, Woolford JL Jr, Gao N. 2017. Structural snapshot of cytoplasmic pre-60S ribosomal particles bound by Nmd3, Lsg1, Tif6 and Reh1. *Nat Struct Mol Biol* **24:** 214–220. doi:10.1038/nsmb.3364

McCaughan UM, Jayachandran U, Shchepachev V, Chen ZA, Rappsilber J, Tollervey D, Cook AG. 2016. Pre-40S ribosome biogenesis factor Tsr1 is an inactive structural mimic of translational GTPases. *Nat Commun* **7:** 11789. doi:10.1038/ncomms11789

Meyer B, Wurm JP, Kotter P, Leisegang MS, Schilling V, Buchhaupt M, Held M, Bahr U, Karas M, Heckel A, et al. 2011. The Bowen–Conradi syndrome protein Nep1 (Emg1) has a dual role in eukaryotic ribosome biogenesis, as an essential assembly factor and in the methylation of Psi1191 in yeast 18S rRNA. *Nucleic Acids Res* **39:** 1526–1537. doi:10.1093/nar/gkq931

Meyer B, Wurm JP, Sharma S, Immer C, Pogoryelov D, Kotter P, Lafontaine DL, Wohnert J, Entian KD. 2016. Ribosome biogenesis factor Tsr3 is the aminocarboxypropyl transferase responsible for 18S rRNA hypermodification in yeast and humans. *Nucleic Acids Res* **44:** 4304–4316. doi:10.1093/nar/gkw244

Mulder AM, Yoshioka C, Beck AH, Bunner AE, Milligan RA, Potter CS, Carragher B, Williamson JR. 2010. Visualizing ribosome biogenesis: parallel assembly pathways for the 30S subunit. *Science* **330:** 673–677. doi:10.1126/science.1193220

Parker MD, Collins JC, Korona B, Ghalei H, Karbstein K. 2019. A kinase-dependent checkpoint prevents escape of immature ribosomes into the translating pool. *PLoS Biol* **17:** e3000329. doi:10.1371/journal.pbio.3000329

Parnell KM, Bass BL. 2009. Functional redundancy of yeast proteins Reh1 and Rei1 in cytoplasmic 60S subunit maturation. *Mol Cell Biol* **29:** 4014–4023. doi:10.1128/mcb.01582-08

Peifer C, Sharma S, Watzinger P, Lamberth S, Kötter P, Entian K-D. 2012. Yeast Rrp8p, a novel methyltransferase responsible for m^1A 645 base modification of 25S rRNA. *Nucleic Acids Res* **41:** 1151–1163. doi:10.1093/nar/gks1102

Peña C, Hurt E, Panse VG. 2017. Eukaryotic ribosome assembly, transport and quality control. *Nat Struct Mol Biol* **24:** 689–699. doi:10.1038/nsmb.3454

Plassart L, Shayan R, Montellese C, Rinaldi D, Larburu N, Pichereaux C, Froment C, Lebaron S, O'Donohue MF, Kutay U, et al. 2021. The final step of 40S ribosomal subunit maturation is controlled by a dual key lock. *Elife* **10:** e61254. doi:10.7554/eLife.61254

Pulicherla N, Pogorzala LA, Xu Z, Farrell HCO, Musayev FN, Scarsdale JN, Sia EA, Culver GM, Rife JP. 2009. Structural and functional divergence within the Dim1/KsgA family of rRNA methyltransferases. *J Mol Biol* **391:** 884–893. doi:10.1016/j.jmb.2009.06.015

Rai J, Parker MD, Huang H, Choy S, Ghalei H, Johnson MC, Karbstein K, Stroupe ME. 2021. An open interface in the pre-80S ribosome coordinated by ribosome assembly factors Tsr1 and Dim1 enables temporal regulation of Fap7. *RNA* **27:** 221–233. doi:10.1261/rna.077610.120

Sanghai ZA, Miller L, Molloy KR, Barandun J, Hunziker M, Chaker-Margot M, Wang J, Chait BT, Klinge S. 2018. Modular assembly of the nucleolar pre-60S ribosomal subunit. *Nature* **556:** 126–129. doi:10.1038/nature26156

Sashital DG, Greeman CA, Lyumkis D, Potter CS, Carragher B, Williamson JR. 2014. A combined quantitative mass spectrometry and electron microscopy analysis of ribosomal 30S subunit assembly in *E. coli*. *Elife* **3:** e04491. doi:10.7554/eLife.04491

Scaiola A, Pena C, Weisser M, Bohringer D, Leibundgut M, Klingauf-Nerurkar P, Gerhardy S, Panse VG, Ban N. 2018. Structure of a eukaryotic cytoplasmic pre-40S ribosomal subunit. *EMBO J* **37:** e98499. doi:10.15252/embj.201798499

Sharma S, Watzinger P, Kötter P, Entian K-D. 2013. Identification of a novel methyltransferase, Bmt2, responsible for the *N*-1-methyl--adenosine base modification of 25S rRNA in *Saccharomyces cerevisiae*. *Nucleic Acids Res* **41:** 5428–5443. doi:10.1093/nar/gkt195

Sharma S, Langhendries JL, Watzinger P, Kötter P, Entian KD, Lafontaine DL. 2015. Yeast Kre33 and human NAT10 are conserved 18S rRNA cytosine acetyltransferases that modify tRNAs assisted by the adaptor Tan1/THUMPD1. *Nucleic Acids Res* **43:** 2242–2258. doi:10.1093/nar/gkv075

Sharma S, Hartmann JD, Watzinger P, Klepper A, Peifer C, Kötter P, Lafontaine DLJ, Entian K-D. 2018. A single N^1-methyladenosine on the large ribosomal subunit rRNA impacts locally its structure and the translation of key metabolic enzymes. *Sci Rep* **8:** 11904. doi:10.1038/s41598-018-30383-z

Strunk BS, Loucks CR, Su M, Vashisth H, Cheng S, Schilling J, Brooks CL III, Karbstein K, Skiniotis G. 2011. Ribosome assembly factors prevent premature translation initiation by 40S assembly intermediates. *Science* **333:** 1449–1453. doi:10.1126/science.1208245

Strunk BS, Novak MN, Young CL, Karbstein K. 2012. A translation-like cycle is a quality control checkpoint for maturing 40S ribosome subunits. *Cell* **150:** 111–121. doi:10.1016/j.cell.2012.04.044

Sturm M, Cheng J, Baßler J, Beckmann R, Hurt E. 2017. Interdependent action of KH domain proteins Krr1 and Dim2 drive the 40S platform assembly. *Nat Commun* **8:** 1–13. doi:10.1038/s41467-017-02199-4

Thomas SR, Keller CA, Szyk A, Cannon JR, Laronde-Leblanc NA. 2011. Structural insight into the functional mechanism of Nep1/Emg1 N1-specific pseudouridine methyltransferase in ribosome biogenesis. *Nucleic Acids Res* **39:** 2445–2457. doi:10.1093/nar/gkq1131

Turowski TW, Lebaron S, Zhang E, Peil L, Dudnakova T, Petfalski E, Granneman S, Rappsilber J, Tollervey D. 2014. Rio1 mediates ATP-dependent final maturation of 40S ribosomal subunits. *Nucleic Acids Res* **42:** 12189–12199. doi:10.1093/nar/gku878

Valášek L, Szamecz B, Hinnebusch AG, Nielsen KH. 2007. In vivo stabilization of preinitiation complexes by formaldehyde cross-linking. *Methods Enzymol* **429:** 163–183. doi:10.1016/S0076-6879(07)29008-1

White J, Li Z, Sardana R, Bujnicki JM, Marcotte EM, Johnson AW. 2008. Bud23 methylates G1575 of 18S rRNA and is required for efficient nuclear export of pre-40S subunits. *Mol Cell Biol* **28:** 3151–3161. doi:10.1128/mcb.01674-07

Woolford JL Jr, Baserga SJ. 2013. Ribosome biogenesis in the yeast *Saccharomyces cerevisiae*. *Genetics* **195:** 643–681. doi:10.1534/genetics.113.153197

Wu S, Tutuncuoglu B, Yan K, Brown H, Zhang Y, Tan D, Gamalinda M, Yuan Y, Li Z, Jakovljevic J, et al. 2016. Diverse roles of assembly factors revealed by structures of late nuclear pre-60S ribosomes. *Nature* **534:** 133–137. doi:10.1038/nature17942

Zorbas C, Nicolas E, Wacheul L, Huvelle E, Heurgue-Hamard V, Lafontaine DL. 2015. The human 18S rRNA base methyltransferases DIMT1L and WBSCR22-TRMT112 but not rRNA modification are required for ribosome biogenesis. *Mol Biol Cell* **26:** 2080–2095. doi:10.1091/mbc.E15-02-0073

MEET THE FIRST AUTHOR

Haina Huang

***Meet the First Author(s)* is a new editorial feature within *RNA*, in which the first author(s) of research-based papers in each issue have the opportunity to introduce themselves and their work to readers of *RNA* and the RNA research community. Haina Huang is the first author of this paper, "The modifying enzyme Tsr3 establishes the hierarchy of Rio kinase binding in 40S ribosome assembly." Haina is a graduate student in the Karbstein laboratory in the Department of Integrative Structural and Computational Biology on the Florida campus of the Scripps Research Institute, with a research focus on dissecting quality control mechanisms during ribosome assembly.**

What are the major results described in your paper and how do they impact this branch of the field?

We show that a conserved rRNA modifying enzyme, Tsr3, coordinates the successive binding of two highly similar kinases, Rio2 and Rio1, to the same location of the assembling small subunit and thereby ensures proper maturation of the subunit. Our work addresses the broader question of how the hierarchy of binding of ribosome assembly factors is established—in this case through an energy-driven process promoted by an rRNA modifying enzyme.

What led you to study RNA or this aspect of RNA science?

Ribosomes are complex macromolecular machines whose assembly requires a machinery of over 200 assembly factors. How cells manage to create a population of correctly folded and uniformly assembled subunits with structural and functional plasticity is just fascinating.

If you were able to give one piece of advice to your younger self, what would that be?

It always takes greater courage to present negative data, disagree and be different.

What are your subsequent near or long-term career plans?

I plan to find an R&D job in industry, ideally focusing on RNA therapeutics. I hope to find a job that can develop novel tools to accelerate both scientific and clinical research processes.